Free-Free Absorption by a Gas Disk in the GPS Radio Galaxy 0108+388

J.M. Marr[1], G.B. Taylor[2] & F. Crawford III[3]

[1] *Union College, Schenectady, NY, USA*
[2] *NRAO, Socorro, NM, USA*
[3] *MIT, Cambridge, MA, USA*

Abstract

We have observed the gigahertz-peaked spectrum source 0108+388 with the VLBA at a range of frequencies above and below the spectral peak. The activity that dominates the radio emission from 0108+388, which is also classified as a Compact Symmetric Object, is thought to be less than 1000 years old. Here we present evidence for a disk of gas in the central tens of parsecs that causes free-free absorption at low frequencies and may have triggered the recent onset of radio frequency activity. The spectral index maps obtained from our observations reveal that the radio spectra of a large area of the map turn over at about the same frequency, indicating that the turnover is due to foreground free-free absorption, rather than synchrotron self-absorption. The morphologies of the spectral index maps further show that the absorbing material is non-uniform and is suggestive of an edge-on disk centered on the core of the active galaxy. A rough model of free-free absorption by a disk of gas that fits the observed opacity maps is obtained.

We have observed the Gigahertz-Peaked Spectrum ("GPS") radio galaxy 0108+388 with the VLBA[1] at two frequencies above the spectral turnover, at the turnover frequency, and at two frequencies below the turnover. The sequence of maps reveal the point-by-point spectra of the radio emission and the morphology of the absorption. If the turnover is due to free-free ("f-f") absorption, one expects the whole source, or large parts of it, to get fainter with decreasing frequencies as the optical depth of the foreground screen increases. If the turnover is due to synchrotron self-absorption (or "SSA"), on the other hand, then small pieces of the source, where the magnetic field and electron density are greatest, will be opaque at higher frequencies and will decrease in intensity with decreasing frequency, while the more diffuse and lower magnetic field parts continue to increase in intensity.

---

[1]The VLBA is operated by the National Radio Astronomy Observatory, which is a facility of the National Science Foundation operated under cooperative agreement by Associated Universities, Inc.
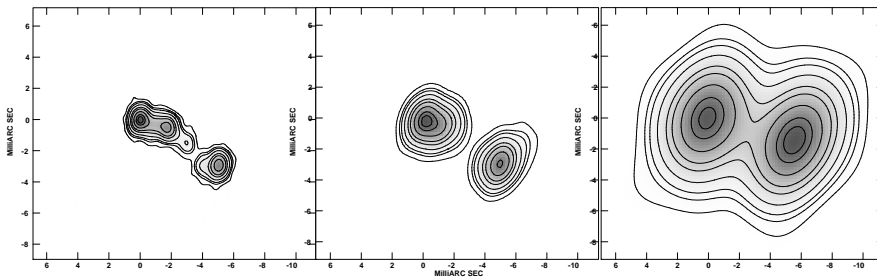
Figure 1: Clean maps at 15.3, 5.0, and 1.7 GHz. The displayed contours correspond to 1, 3, 5, 10, 20, 30, 50, 75, and 90% of the peak flux densities, which are 0.130, 0.396, and 0.221 Jy/beam, respectively.
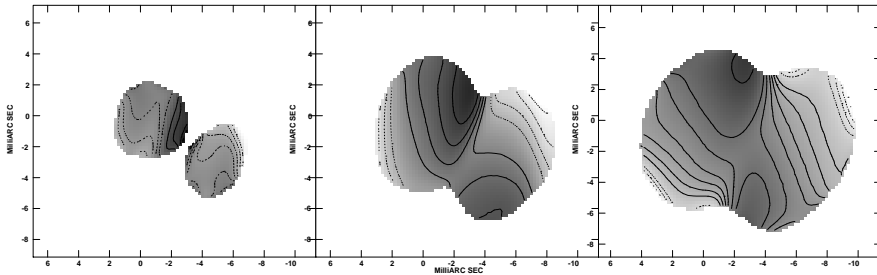

Figure 2: Spectral Index Maps between: 15.3 and 8.4 GHz, 8.4 and 5.0 GHz, 5.0 and 2.7 GHz, and 2.7 and 1.3 GHz. The contours represent spectral index values of -3, -2, -1.6, -1.2, -0.9, -0.6, -0.3, $+0.3$, 0.6, 0.9, 1.2, 1.6, 2.0, and 3.0, where $F_\nu \propto \nu^\alpha$.

Observations were made at 8.415, 4.983, 2.267, and 1.663 GHz on 24 June 1996 and at 15.349 and 8.415 GHz on 3 February 1997. The CLEAN maps at 15.3, 8.4, and 1.7 GHz are displayed in Fig. 1.

Spectral index maps between neighboring frequency bands were made from data sets that were edited to yield identical resolutions. The three lower frequency spectral index maps are shown in Fig. 2. The spectral index map between the two highest frequencies, not shown, is consistent with that found by Taylor et al. (1996); the two major components have steeply declining spectra and a small component in the middle, inferred to be the core, has an inverted spectrum. In the spectral-index map between 8.4 and 5.0 GHz, the spectra of the inner regions of the two major components are flatter, but the outer regions are still steeply inverted. Between 5.0 and 2.3 GHz, the spectra of all but the easternmost and westernmost edges are inverted. Between 2.3 and 1.7 GHz, the spectral index map looks similar to that between 2.3 and 5.0 GHz, except that the spectral indices are larger and the region

of inverted spectra encompasses almost the whole source. In both of the two lower frequency spectral index maps the region with inverted spectra appears to run across the map in the north-south direction. The most steeply inverted spectra are located in two areas north and south of the core at the edge of the mapped region.

The turnover of the composite spectrum at 5.0 GHz clearly results from the majority of the source turning over at this frequency. This is in conflict with the expectations for SSA but is consistent with f-f absorption by foreground gas. Additionally, the peak spectral index is 3.2, which is sufficiently greater than the maximum allowable spectral index with SSA. The general character of the spectral index distributions is also suggestive of an edge-on disk centered on the core.

To directly map the absorbing gas we made opacity maps. The creation of the opacity maps involves comparison of maps at all the observed frequencies (as described below), so we edited all data sets to have the same (u,v) range. These truncated data sets had aspect ratios of only 9.0 but the resulting maps still had good fidelity; the final maps look very much like the 2.3 and 1.7 GHz clean maps made with the full data sets and the signal to noise ratios are higher. The fidelity of these maps result because the structure of this source is quite simple.

At each point in the map, we use the spectral index between 15.3 and 8.4 GHz to extrapolate the flux densities at 8.4 GHz to the lower frequencies. This produces reasonable estimates of the flux densities at 2.3 and 1.7 GHz in the absence of the absorbing medium. The optical depths at each point in the map at 2.3 and 1.7 GHz are then inferred by comparing the observed flux-densities with the extrapolated flux-densities. However, since the optical depths at 8.4 GHz are not really zero, the extrapolation of the spectrum produces a small error. We improve the inferred optical depths by iterating the procedure. The inferred optical depths at 2.3 and 1.7 GHz are used to infer the optical depths at 8.4 and 15.3 GHz (assuming f-f absorption), which are then used to correct the 8.4 and 15.3 GHz maps to produce maps of the unabsorbed flux-densities. These modified maps are then used to recreate the 1.7 and 2.3 GHz maps of the unabsorbed flux-densities, which are used, in turn, in the creation of improved opacity maps.

The resultant opacity maps at 2.3 and 1.7 GHz are shown in Fig. 3. These maps show that the maximum absorption occurs at two points north and south of the center and that the absorbing medium is extended in the north-south direction, roughly perpendicular to the jet axis.
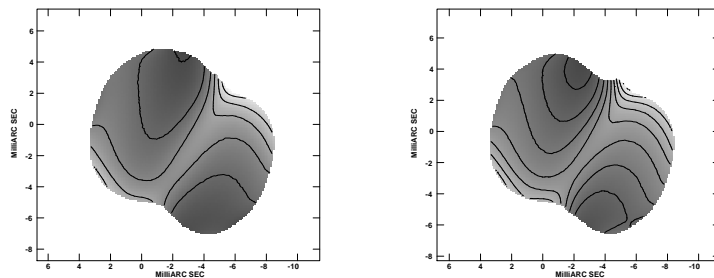
Figure 3: Opacity maps at 2.7 GHz and 1.3 GHz. The contours represent optical depths of 0.4, 0.8, 1.2, 1.6, 2.0, 2.4, 2.8, 3.2 and 3.6.
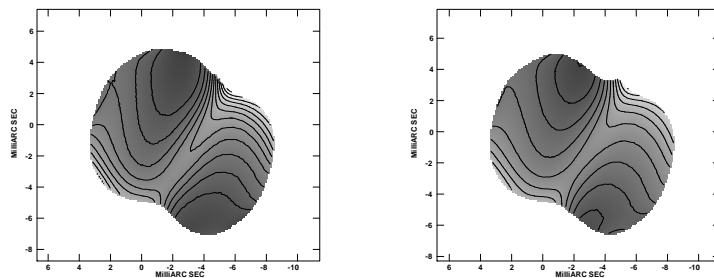

Figure 4: Maps of $\tau_\nu \times \nu^{2.1}$ at 2.7 and 1.3 GHz. The displayed contours represent values of 1, 2, 3, 4, 5, 6, 7, 8, 9, 10, 11, and 12.

To check for consistency in the f-f model we remove the frequency dependence in our two opacity maps (by multiplying by $\nu^{2.1}$). These maps, shown in Fig. 4, are essentially identical, indicating that f-f absorption fits the spectrum at each point in the map.

Using the maps in Fig. 4 we roughly model the size and conditions of the absorbing medium. We find the maps fit a disk of gas with radius ≈ 180 pc, $\langle N_e \rangle \approx 600\,\mathrm{cm}^{-3}$, and $\langle T_e \rangle \approx 10^4 \mathrm{K}$. Comparing to the HI absorption results of Carilli et al. (1998) we estimate a ratio of the column depths of $\langle N_e \rangle$ to N_{HI} of $\frac{3500}{T_S}$, where T_S is the spin temperature of the HI atoms.

References

Carilli, C.L., Menten, K.M., Reid, M.J. et al. 1998, *ApJ*, **494**, 175

Taylor, G.B., Readhead, A.C.S., & Pearson, T.J. 1996, *ApJ*, **463**, 95